of the cortex, hippocampus, hypothalamus and cerebellum of transgenic animals[11]. The familial AD mutation at residue 717[12] may be important as it partially shifts production of Aβ from the 40-amino-acid form to the more amyloidogenic 42-residue peptide known to predominate in plaques[16,17]. Preparation of APP transgenic mice independently harbouring each of these features will be required to identify the essential component(s) that result in pathology.

The most notable feature of these transgenic mice is their Alzheimer-like neuropathology, which includes extracellular Aβ deposition, dystrophic neuritic components, gliosis and loss of synaptic density with regional specificity resembling that of AD. Based on the limited sampling to date, plaque density appears to increase with age in these transgenic mice, as it does in humans[1], implying a progressive Aβ deposition that exceeds its clearance, as also proposed for AD[18]. Our transgenic model provides strong new evidence for the primacy of APP expression and Aβ deposition in AD neuropathology and offers a means to test whether compounds that lower Aβ production and/or reduce its neurotoxicity *in vitro* can produce beneficial effects in an animal model prior to advancing such drugs into human trials. □

Received 17 October 1994; accepted 5 January 1995.

1. Selkoe, D. J. *A. Rev. Neurosci.* **17,** 489–517 (1994).
2. Hardy, J. *Clin. geriatr. Med.* **10,** 239–247 (1994).
3. Mann, D. M. A. *et al. Neurodegeneration* **1,** 201–215 (1992).
4. Quon, D. *et al. Nature* **352,** 239–241 (1991).
5. Sanhu, F. A., Salim, M. & Zain, S. B. *J. biol. Chem.* **266,** 21331–21334 (1991).
6. Lamb, B. T. *et al. Nature Genet.* **5,** 22–30 (1993).
7. Pearson, B. E. & Choi, T. K. *Proc. natn. acad. Sci. U.S.A.* **90,** 10578–10582 (1993).
8. Mucke, L. *et al. Brain Res.* **666,** 151–167 (1994).
9. McConlogue, L. *et al. Neurobiol. Aging* **15,** S12 (1994).
10. Higgins, L. S. *et al. Ann. Neurol.* **35,** 598–607 (1994).
11. Sasahara, M. *et al. Cell* **64,** 217–227 (1991).
12. Murrell, J. *et al. Science* **254,** 97–99 (1991).
13. Seubert, P. *et al. Nature* **359,** 325–327 (1992).
14. Cork, L. C. *et al. J. Neuropath. exp. Neurol.* **47,** 629–641 (1988).
15. Masliah, E. *et al. Am. J. Path.* **138,** 235–246 (1991).
16. Suzuki, N. *et al. Science* **264,** 1336–1340 (1994).
17. Roher, A. *et al. J. biol. Chem.* **269,** 3072–3083 (1993).
18. Maggio, J. E. *et al. Proc. natn Acad. Sci. U.S.A.* **89,** 5462–5466 (1992).
19. Hogan, B., Constantini, F. & Lacey, E. in *Manipulating the Mouse Embryo: A Laboratory Manual* (Cold Spring Harbor Laboratory, Cold Spring Harbor, NY, 1986).
20. Chomazynski, P. & Sacchi, N. *Analyt. Biochem.* **162,** 156–159 (1987).
21. Wang, A. M. *et al. Proc. natn. Acad. Sci. U.S.A.* **86,** 9717–9721 (1989).
22. Oltersdorf, T. *et al. J. biol. Chem.* **265,** 4492–4497 (1990).
23. Arai, H. *et al. Proc. natn. Acad. Sci. U.S.A.* **87,** 2249–2253 (1990).
24. Tamaoka, A. *et al. Proc. natn. Acad. Sci. U.S.A.* **89,** 1345–1349 (1992).
25. Games, D. *et al. Neurobiol. Aging* **13,** 569–576 (1992).
26. Saido, T. C. *et al. J. biol. Chem.* **269,** 15253–15257 (1994).
27. Dickson, D. W. *et al. Acta neuropath.* **79,** 486–493 (1990).
28. Masliah, E. *et al. J. Neuropath. exp. Neurol.* **52,** 619–632 (1993).
29. Masliah, E. *et al. Acta neuropath.* **81,** 428–433 (1991).

ACKNOWLEDGEMENTS. We thank M. Mallory, A. Maya, N. Ge, E. Rockenstein, O. Stephenson and E. Johnstone for technical assistance; the animal care technicians involved in this project; J. Trojanowski for human brain sections; T. Saido and D. Selkoe for anti-Aβ antibodies 9204 and R1280, respectively; T. Collins and D. Goldgaber for the PDGF promoter and APP cDNA subclones, respectively; and D. Selkoe for helpful comments and advice.

Gating of the voltage-dependent chloride channel ClC-0 by the permeant anion

Michael Pusch, Uwe Ludewig, Annett Rehfeldt* & Thomas J. Jentsch†

Centre for Molecular Neurobiology (ZMNH), Hamburg University, Martinistrasse 52, D-20246 Hamburg, Germany

CHLORIDE channels of the ClC family are important for the control of membrane excitability[1–3], cell volume regulation[4,5], and possibly transepithelial transport[6,7]. Although lacking the typical voltage-sensor found in cation channels[8–10], gating of ClC channels is clearly voltage-dependent. For the prototype *Torpedo* channel ClC-0 (refs 11–15) we now show that channel opening is strongly facilitated by external chloride. Other less permeable anions can substitute for chloride with less efficiency. ClC-0 conductance shows an anomalous mole fraction behaviour with Cl^-/NO_3^- mixtures, suggesting a multi-ion pore. Gating shows a similar anomalous behaviour, tightly linking permeation to gating. Eliminating a positive charge at the cytoplasmic end of domain D12 changes kinetics, concentration dependence and halide selectivity of gating, and alters pore properties such as ion selectivity, single-channel conductance and rectification. Taken together, our results strongly suggest that in these channels voltage-dependent gating is conferred by the permeating ion itself, acting as the gating charge.

The *Torpedo* electric organ Cl^--channel ClC-0 (ref. 12) has a 'slow' gate operating on both protochannels of the double-barrelled channel[13,14] simultaneously, and a 'fast' gate acting on single protochannels[13–15]. Both gates have opposite voltage-dependence, with the fast gate being opened by depolarization. ClC-0 was expressed in *Xenopus* oocytes and the fast gate was studied in isolation (Fig. 1*a*). The dependence of the steady-state open probability, p_{open}, on the transmembrane voltage V can be described by the Boltzmann distribution $p_{open} = 1/(1+\exp(z_n e_0(V_{1/2}-V)/kT))$ (where e_0 is the elementary charge, $V_{1/2}$ is the voltage of half-maximal activation, k is the Boltzmann constant, and T is the temperature) with a nominal gating charge $z_n \sim 1$ in agreement with earlier data[13,14]. Consistent with single-channel measurements[13,14], gating kinetics indicate a two-state gating mechanism. Reducing extracellular Cl^- concentration ($[Cl^-]_0$) shifts $p_{open}(V)$ to positive voltages without significantly changing its slope (the gating charge) (Fig. 1*b*). In contrast, intracellular chloride has little effect (Fig. 1*c*). A dependence of ClC-0 microscopic gating transitions on the Cl^--gradient has already been noted[15].

The dependence of gating on $[Cl^-]_0$ could be due to a simple mechanism in which channel opening depends on chloride binding to a site within the pore; p_{open} should then increase with $[Cl^-]_0$ and with positive intracellular potentials. Intracellular chloride has little effect on gating, because it cannot reach its binding site in the closed state.

The simplest model assumes that chloride-binding to a single site in the pore is required for channel opening[10]. Although it may serve as a first approximation to our data, the shift of p_{open} with $[Cl^-]_0$ is ~20% less than minimally predicted[10]. This suggests that this model is either principally unsuited to explain ClC-0 gating, or that it needs further refinement.

The pores of many channels, including certain chloride channels[16], can accommodate more than one ion, leading to concentration-dependent interactions within the pore. In a single-ion pore, conductance changes monotonously when the concentration ratio between two permeant ionic species is varied; in a multi-ion pore, however, interactions between different species can lead to a current minimum at a certain concentration ratio, an 'anomalous mole fraction behaviour'[16,17]. We indeed found this effect with mixtures of Cl^- and NO_3^- (Fig. 2*b*), indicating that ClC-0 has a multi-ion pore. Thus, a model having a single chloride-binding site[10] may be too simplistic.

* Deceased.
† To whom correspondence should be addressed.

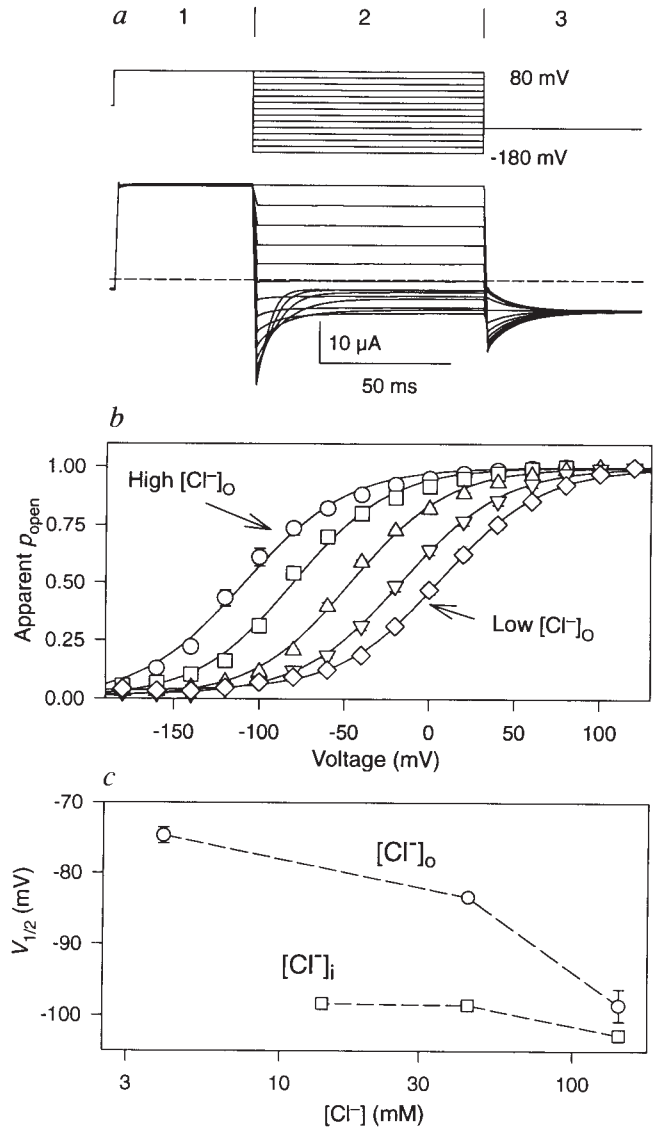

FIG. 1 Voltage- and Cl -dependent gating of ClC-0 (WT). *a*, Voltage-clamp protocol and current traces used to study the fast gate and the instantaneous *I–V* of ClC-0. To study the fast gate in isolation, the slow gate is maximally activated by previous hyperpolarization (not shown) and remains open during the pulse programme. Clamping to +80 mV (part 1) maximally opens the fast gate. Then deactivating currents are measured at different test voltages (period 2). Extrapolation to the beginning of period 2 yields instantaneous *I–V* of the open channel (see Fig. 4). Then p_{open} is monitored at the constant test pulse to −100 mV by extrapolating currents to the beginning of period 3. *b*, Steady-state voltage-dependence of the fast gate of ClC-0 expressed in oocytes at different $[Cl^-]_o$ (○, 100 mM; □, 21.5 mM; △, 4.6 mM; ▽, 1 mM; ◇, 0.22 mM). The high Cl^- solution contained 100 mM NaCl, 5 mM $MgSO_4$ and 5 mM Ca–HEPES, pH 7.4. $[Cl^-]$ was lowered by replacing it with an equiosmolar amount of sucrose. Gating is not affected if extracellular sodium is replaced by potassium or *N*-methyl-D-glucamine. *c*, Half-maximal activation voltage ($V_{1/2}$) of ClC-0 expressed in CHO cells at different external and internal $[Cl^-]$ (obtained by equilibration with the patch pipette solution).

METHODS. Capped cRNA was transcribed from ClC-0 (ref. 12) and injected into *Xenopus* oocytes as described[12,4]. Currents were measured after 1–3 days using two-electrode voltage-clamp and pCLAMP5.5 software. Averaged data from 5 oocytes is shown. Apparent p_{open} was obtained by driving the fast gate into steady-state at various voltages (*a*, part 2), and then measuring the peak current (where p_{open} has not yet changed) at a constant test-potential (*a*, part 3). Gating relaxations were slow enough compared to capacitative transients to extrapolate reliably a single exponential function to the onset of the test pulse (*a*, part 3). Apparent p_{open} was normalized to the maximum current flowing after positive pre-potentials. As p_{open} is measured at a constant test potential, it is independent of single-channel *I–V*. CHO cells were stably transfected with ClC-0 cloned into pcDNAI-neo and selected with G418. Currents in CHO cells were measured using the whole-cell and outside-out configuration of the patch-clamp technique. External solutions were 135 mM NaCl, 5 mM KCl, 1.8 mM $CaCl_2$, 1 mM $MgCl_2$, 5 mM Na–HEPES. Internal solutions contained 140 mM KCl, 10 mM EGTA, 5 mM K–HEPES and 2 mM $MgCl_2$. Cl was reduced by substitution with equal amounts of cyclamate. Data represent mean values of 2 patches for variation of external, and >10 patches for internal chloride. Error bars are s.e.m. throughout.

If the permeant anion directly gates the channel, one may expect that p_{open} will also show an anomalous mole-fraction behaviour. Indeed $V_{1/2}$ (the voltage at which $p_{open} = 0.5$) has a minimum at nearly the same mole fraction (Fig. 2*b*).

To identify structures involved in gating, we neutralized all charged residues in putative transmembrane spans (Fig. 3*a*). Except for a lysine towards the end of domain D12, the mutants could either not be expressed functionally, or were indistinguishable from wild type (WT). Gating and permeation were altered in mutants K519Q, K519E and K519H, which yielded very similar currents. K519R was intermediate to WT. Thus, a positive charge and other features of the side chain are important at this position. Mutants in K520 and in residues 515 to 518 resembled WT, demonstrating the specificity of K519. We concentrated on K519E. Its gating is slower (Fig. 3*b*) but still depends on $[Cl^-]_o$ (Fig. 3*c*). The nominal gating charge remains ~1. In contrast to WT, K519E currents do not deactivate completely at negative voltages, but the apparent p_{open} deduced from macroscopic currents saturates at ~35% (Fig. 3*c*). This does not result from a nonspecific leak current, but is due to a low conductance state of the channel (~0.3 pS) remaining with closed fast gates (our manuscript in preparation).

Several pore properties are also changed. Although the instantaneous *I–V* of WT ClC-0 Cl^--currents is linear[13,14], it is outwardly rectifying with K519E (Fig. 4*a*, *b*). This agrees with the assumed cytoplasmic location of K519 and with effects described for mutations close to pore entrances in other channels[18]. Noise analysis[19,20] indicates that single-channel conductance was reduced from ~8 pS (WT) to between ~0.8 (at −140 mV) and ~3 pS (at +60 mV) for K519E, making single-channel studies unfeasible. Cl^- permeates WT ClC-0 better than Br^- and NO_3^-, and I^- blocks it (Fig. 4*a*). K519E, however, conducts Br^- as well as Cl^-, NO_3^- conductance is increased, and I^- block reduced (Fig. 4*b*). If our model is correct, one may expect that this difference in halide selectivity of conductance entails a difference in the halide selectivity of gating, because the anion must penetrate the ion-selective pore to reach its binding site. Both in WT and K519E ClC-0, gating is stimulated by Cl^-, Br^-, and NO_3^- or I^- (in comparison to glutamate or other impermeant anions) (Fig. 4*c*, *d*). This suggests that only permeant ions directly affect gating. Although WT ClC-0 is gated less efficiently (in comparison to Cl^-) with Br^- and especially I^- (Fig. 4*c*), this difference is indeed reduced in the less selective mutant K519E (Fig. 4*d*). K519E does not abolish the multi-ion behaviour, but shifts the conductance maximum to a different mole fraction (Fig. 2*c*). With both WT and K519E, p_{open} depends less steeply on voltage with NO_3^- as compared to Cl^-.

In voltage-dependent cation channels, pores and voltage-sensors are assigned to different structures[8,10,17,21,23], even though several point mutations change both gating and

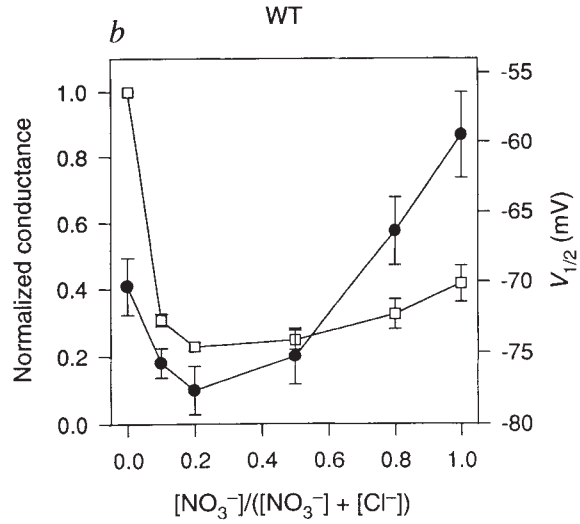

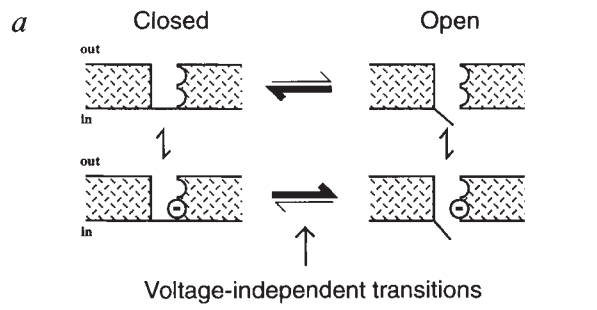

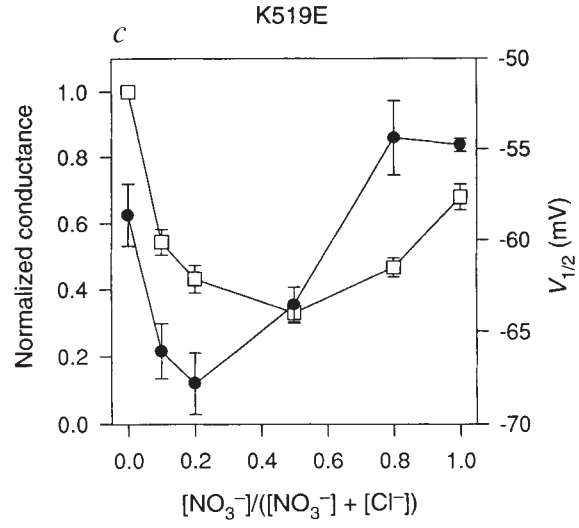

FIG. 2 Schematic model of fast Cl⁻-dependent gating of ClC-0 (*a*) and anomalous mole fraction behaviour resulting from interactions in the pore (*b*, *c*). The model in *a* assumes intrinsically voltage-independent gating transitions. The pore contains two anion-binding sites, and the gate is close to its cytoplasmic mouth. Occupation of the internal binding site shifts the equilibrium between closed and open conformations to the open state, irrespective of whether the outer binding site is occupied (for simplicity, occupation of outer binding site is not shown). This leads to a voltage- and concentration-dependence of gating. Binding of an anion to one site can influence the binding of a second anion to the other site (for example, by electrostatic interaction). This can account for the anomalous mole fraction effect when both NO_3^- and Cl^- arepresent. This interaction is also able to explain the shallower voltage-dependence of gating with NO_3^-; in this case, the transition of NO_3^- from the outer to the inner binding site makes the major contribution to the voltage-dependence. *b*, c, Anomalous mole fraction behaviour of conductance (□) and of gating (●); $V_{1/2}$ is the voltage where $p_{open} = 0.5$) for WT ClC-0 (*b*) and the K519E mutant (c). Similar effects were found with Br^-/NO_3^- mixtures, but no anomalous mole fraction behaviour was found in Cl^-/Br^-, Cl /I , or Br /I mixtures.

METHODS. Channels were expressed and measured in oocytes as described in Fig. 1. The different mole fractions were obtained by replacing NaCl with equal amounts of $NaNO_3$ in a solution containing 100 mM NaCl and 5 mM Ca–HEPES pH 7.4. Conductance was measured as slope conductance at +60 mV. $V_{1/2}$ was obtained by Boltzmann fits to steady-state p_{open}. Values represent mean values from 4 oocytes. Error bars indicate s.e.m.

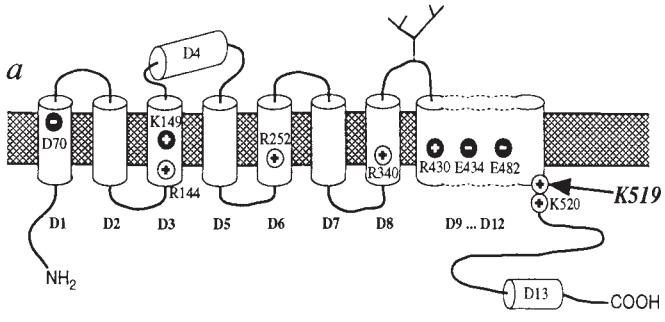

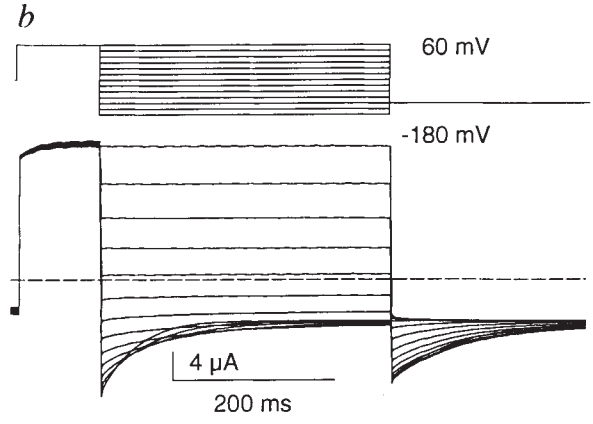

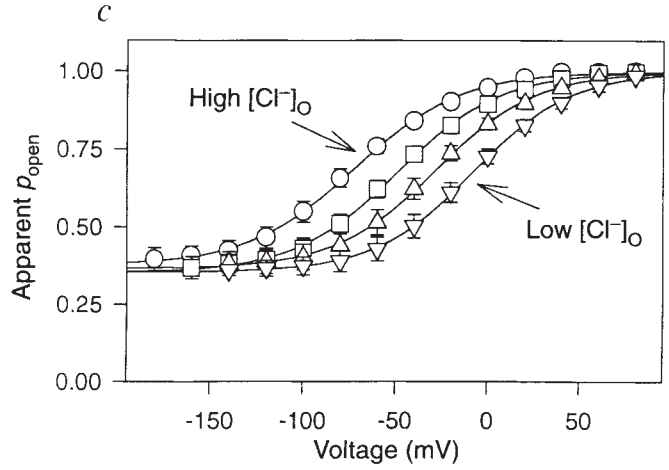

FIG. 3 Location of mutated residues (*a*) and properties of mutant K519E (*b*–c). *a*, Location of charged residues that were mutated to glutamine (K519 also to E, H and R). Mutants that could not be expressed functionally are indicated by filled symbols (D70, K149, R430, E434, E482). R144Q, R252Q, R340Q and K520Q were indistinguishable from WT (open symbols). K519 is conserved in ClC-0, −1, −2 and the ClC-K proteins. We also mutated non-charged residues N-terminal to K519, which gave essentially WT currents (I515L, I516L, Q517R, I518L; not shown in model). Glycosylation studies[7], low homology in D4, and the apparent importance of K149 led us to revise the originally proposed transmembrane model[1,2,5]. There may be several transmembrane spans in the broad hydrophobic region D9–D12, the exact topology of which is unknown. The region after D12 is cytoplasmic[5]. *b*, Voltage-clamp traces of K519E expressed in oocytes. Note the difference in time scale compared to Fig. 1*a* (for explanation of pulse protocol, see there). *c*, Steady-state p_{open} as a function of voltage and $[Cl^-]_o$. Chloride concentrations are as in Fig. 1*b*, except that no measurements were done with 0.22 mM Cl^- (because of the low conductance of K519E). The scale gives 'apparent p_{open}' as calculated from macroscopic current measurements (see Fig. 1a), which differs from true p_{open} because of a residual conductance remaining with closed fast gates ('leaky closed state'). Data are averaged from 5 oocytes.

METHODS. Mutations were introduced by recombinant PCR and verified by sequencing. To boost expression, K519E was cloned into a vector containing *Xenopus* globin untranslated sequences[29]. cRNA was prepared and functionally analysed as in Fig. 1.

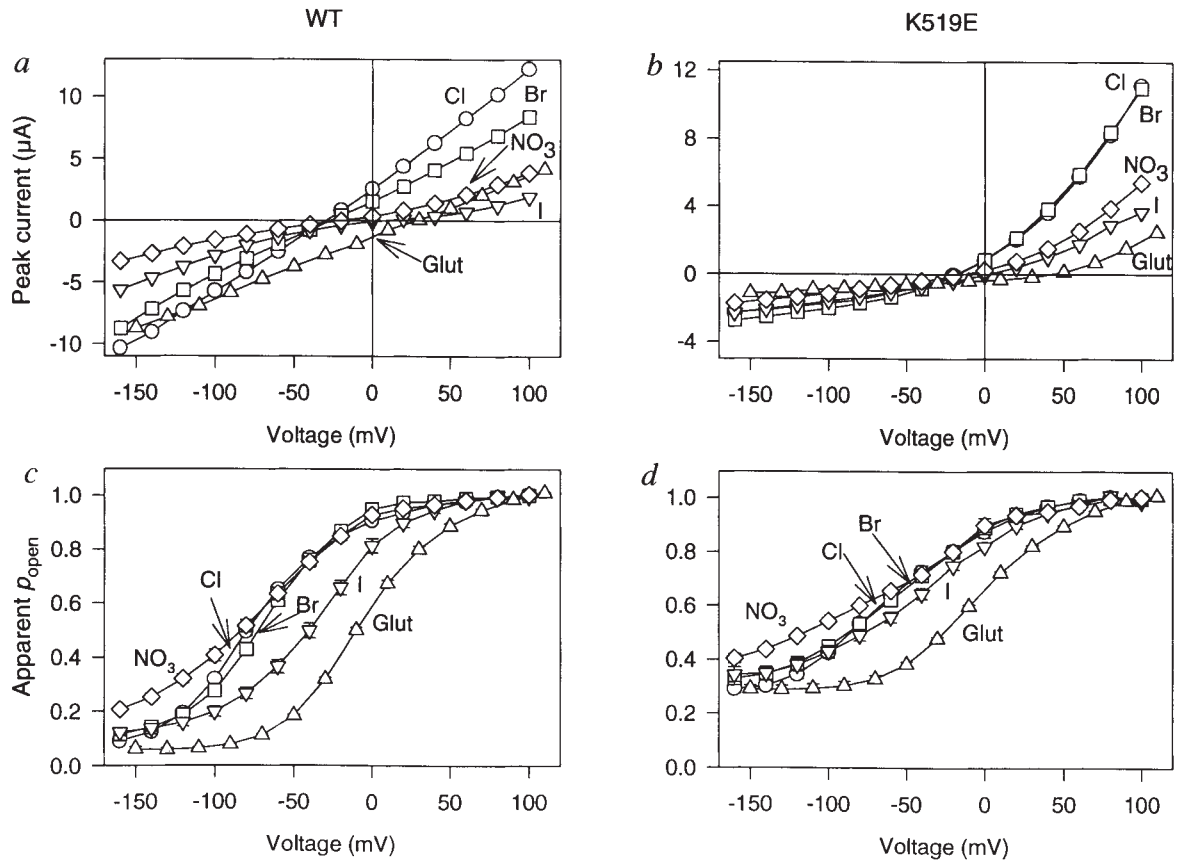

FIG. 4 Halide selectivity of conduction (*a*, *b*) and of gating (*c*, *d*) of WT and K519E ClC-0, respectively. *a*, *b*, Instantaneous (open channel) *I–V* of WT ClC-0 and mutant K519E, respectively, measured in ND96 (104 mM Cl) (ref. 4) (○), or in ND96 in which 96 mM of Cl^- were substituted by Br^- (□), NO_3^- (◇), I^- (▽) or glutamate (△) (this leaves 8 mM Cl in the solution). Note the strong outward rectification and relative loss of selectivity of K519E. *c*, *d*, Halide selectivity of gating for WT and K519E ClC-0, respectively. Apparent p_{open} was determined as described in Fig. 1*a* using the solutions described for *a*, *b*. Aspartate, cyclamate, gluconate, methanesulphonate and sulphate were also unable to permeate and to increase p_{open} (results not shown). As in Fig. 3c, 'apparent p_{open}' of K519E saturates at ~0.35 and is different from 'true' p_{open} because of the 'leaky closed state'.

METHODS. Channels were expressed and analysed in oocytes essentially as described in Fig. 1. The linear *I–V* of open ClC-0 has been described[13,14]. The outward rectification of K519E is also supported by our noise analysis (~0.8 pS at −140 mV, and ~3 pS at +60 mV, our manuscript in preparation), and by macroscopic currents in cell-attached patches which provide higher time-resolution. For *a* and *b*, representative measurements done on a single oocyte are shown; in c and *d*, data from 3 oocytes were averaged.

conductance[24,25]. The influences permeant ions can have on gating of these channels are generally classified as modulatory effects on intrinsically voltage-dependent conformational changes[17]. This work suggests a fundamentally different gating mechanism for ClC-0, in which gating is intrinsically linked to permeation. Although a very simple model[10] involving a single anion-binding site in the pore describes gating to a first approximation, the anomalous mole fraction behaviour suggests more than one binding site in the pore (Fig. 2*a*). Only occupation of the internal site is postulated to affect gating. Binding of chloride to either site influences binding of a second ion to the other site, explaining both the anomalous mole fraction behaviour and the shallower slope seen with NO_3^-. Preliminary model calculations show that it can indeed describe ClC-0 gating (our manuscript in preparation).

In addition to the strong dependence of gating on $[Cl^-]_o$, several findings provide independent strong support for this model. (1) Only permeant anions affect gating. (2) A specific mutation (K519E) affects both conduction and gating. (3) The ion selectivity of conduction is reflected in the ion selectivity of gating; in the mutant, ion selectivities of conduction and gating vary roughly in parallel, as expected when the gating anion has to penetrate the ion-selective pore to reach its binding site. (4) With NO_3^-, p_{open} depends less steeply on V; this can be explained by interactions between the two binding sites. (5) With Cl^-/NO_3^- mixtures, conduction shows an anomalous mole fraction behaviour (strictly a pore property), which is reflected in a similar behaviour of gating.

Findings (3) to (5) are nearly impossible to reconcile with the most simple alternative model in which anion binding to an external site modulates intrinsically voltage-dependent gating. However, they are naturally explained in the framework of our model (Fig. 2*a*), for which they provide very strong support.

K519 is probably located at the intracellular end of the pore where both conduction and gating are controlled. Though tempting, it is not possible to conclude that it directly is the internal anion binding site. In agreement with our results, an alignment[26] of ClC-0 with vastly different cation and anion channels suggests that the D9-D12 segment may participate in permeation, though homology is very weak. Gating models similar to ours may also apply for other ion channel classes. For instance, gating of inwardly rectifying K^+ channels, which also lack the voltage-sensor motif[27], depends on extracellular potassium[27,28]. □

Received 12 August; accepted 16 December 1994.

1. Steinmeyer, K. *et al. Nature* **354,** 304–308 (1991).
2. Koch, M. C. *et al. Science* **257,** 797–800 (1992).
3. Steinmeyer, K., Lorenz, C., Pusch, M., Koch, M. C. & Jentsch, T. J. *EMBO J.* **13,** 737–743 (1994).

4. Thiemann, A., Gründer, S., Pusch, M. & Jentsch, T. J. *Nature* **356,** 57–60 (1992).
5. Gründer, S., Thiemann, A., Pusch, M. & Jentsch, T. J. *Nature* **360,** 759–762 (1992).
6. Uchida, S. *et al. J. biol. Chem.* **268,** 3821–3824 (1993).
7. Kieferle, S., Fong, P., Bens, M., Vandewalle, A. & Jentsch, T. J. *Proc. natn. Acad. Sci. U.S.A.* **91,** 6943–6947 (1994).
8. Stühmer, W. *et al. Nature* **339,** 597–603 (1989).
9. Papazian, D. M., Timpe, L. C., Jan, Y. N. & Jan, L. Y. *Nature* **349,** 305–310 (1991).
10. Sigworth, F. J. *Q. Rev. Biophys.* **27,** 1–40 (1994).
11. White, M. M. & Miller, C. *J. biol. Chem.* **254,** 10161–10166 (1979).
12. Jentsch, T. J., Steinmeyer, K. & Schwarz, G. *Nature* **348,** 510–514 (1990).
13. Hanke, W. & Miller, C. *J. gen. Physiol.* **82,** 25–45 (1983).
14. Bauer, C. K., Steinmeyer, K., Schwarz, J. R. & Jentsch, T. J. *Proc. natn. Acad. Sci. U.S.A.* **88,** 11052–11056 (1991).
15. Richard, E. A. & Miller, C. *Science* **247,** 1208–1210 (1990).
16. Tabcharani, J. A. *et al. Nature* **366,** 79–82 (1993).
17. Hille, B. *Ionic Channels of Excitable Membranes* (Sinauer, Sunderland, MA, 1992).
18. Imoto, K. *et al. Nature* **335,** 645–648 (1988).
19. Heinemann, S. H. & Conti, F. *Meth. Enzym.* **207,** 131–148 (1992).
20. Pusch, M., Steinmeyer, K. & Jentsch, T. J. *Biophys. J.* **66,** 149–152 (1994).
21. Yool, A. J. & Schwarz, T. L. *Nature* **349,** 700–704 (1991).
22. Hartmann, H. A. *et al. Science* **251,** 942–944 (1991).
23. Heinemann, S. H., Terlau, H., Stühmer, W., Imoto, K. & Numa, S. *Nature* **356,** 441–443 (1992).
24. Kirsch, G. E. *et al. Neuron* **8,** 499–505 (1992).
25. Heginbotham, L., Lu, Z., Abramson, T. & MacKinnon, R. *Biophys. J.* **66,** 1061–1067 (1994).
26. Jan, L. Y. & Jan, Y. N. *Nature* **371,** 119–122 (1994).
27. Kubo, Y., Baldwin, T. J., Jan, Y. N. & Jan, L. Y. *Nature* **362,** 127–133 (1993).
28. Hagiwara, S., Miyazaki, S. & Rosenthal, N. P. *J. gen. Physiol.* **67,** 621–638 (1976).
29. Krieg, P. A. & Melton, D. A. *Nucleic Acids Res.* **12,** 7057–7070 (1984).

ACKNOWLEDGEMENTS. We thank C. Schmekal for technical assistance. This work was supported, in part, by the Bundesministerium für Forschung und Technologie, the Deutsche Forschungsgemeinschaft, the Fonds der Chemischen Industrie and the US Cystic Fibrosis Foundation.

Expression of *relB* is required for the development of thymic medulla and dendritic cells

Linda Burkly*, Catherine Hession*, Lynn Ogata†, Christina Reilly†, Lori Anne Marconi†, Dian Olson*, Richard Tizard*, Richard Cate* & David Lo†‡

* Biogen Inc., Cambridge, Massachusetts 02142, USA
† Department of Immunology, The Scripps Research Institute, La Jolla, California 92037, USA

DENDRITIC cells (DC) derived from bone marrow are critical in the function of the immune system, for they are the primary antigen-presenting cells in the activation of T-lymphocyte response. Their differentiation from precursor cells has not been defined at a molecular level, but recent studies have shown an association between expression of the *relB* subunit of the NF-κB complex[1–5] and the presence of DC in specific regions of normal unstimulated lymphoid tissues[4–6]. Here we show that *relB* expression also correlates with differentiation of DC in autoimmune infiltrates *in situ*, and that a mutation disrupting the *relB* gene results in mice with impaired antigen-presenting cell function, and a syndrome of excess production of granulocytes and macrophages. Thymic *UEA-1*$^+$ medullary epithelial cells from normal mice show striking similarities to DC and, interestingly, these cells are also absent in *relB* mutant mice. Taken together, these results suggest that *relB* is critical in the coordinated activation of genes necessary for the differentiation of two unrelated but phenotypically similar cells (DC and thymic *UEA-1*$^+$ medullary epithelial cells) and is therefore a candidate for a gene determining lineage commitment in the immune system.

Although *relB* expression can be found in B-cell enriched fractions[4,5], recent studies using *in situ* hybridization and immunostaining showed stronger expression specifically associated with DC in lymphoid tissues[6], suggesting a role for *relB* in the development of DC from bone marrow precursors. Consistent with this, analysis of islet lymphoid infiltrates in a model of autoimmune diabetes revealed expression of *relB* within the DC-containing regions (Fig. 1*b*, *c*) and not among the functionally related macrophages (Fig. 1*a*), suggesting that *relB* expression correlates with new induction of DC differentiation.

Direct evidence for a relationship between *relB* and DC differentiation was found in mice with an insertional mutation in the *relB* gene, inactivating its expression. This mutation was caused by chance integration of a class I major histocompat-

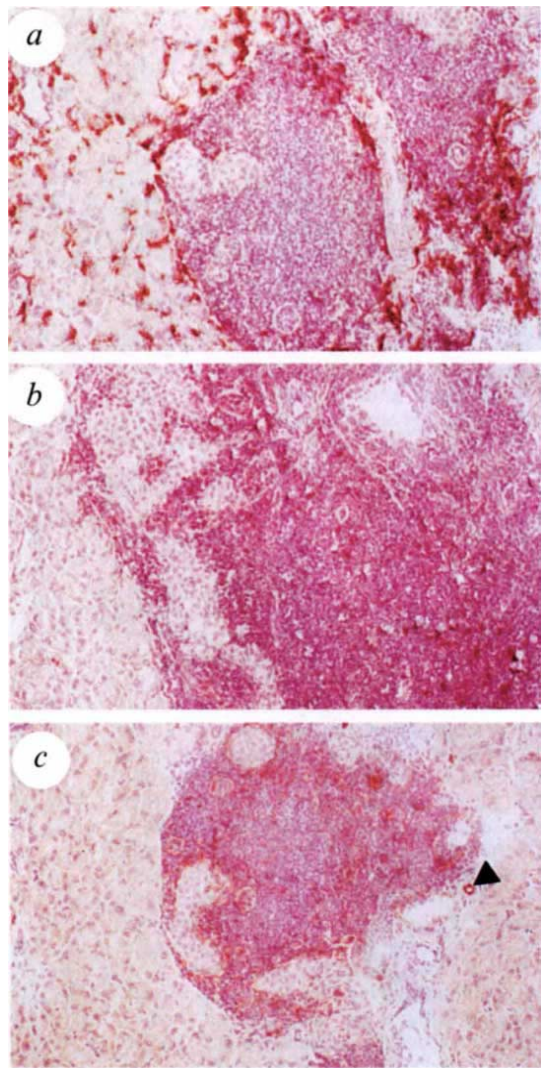

FIG. 1 Histology of inflammation in pancreatic islets. *a*, Stained for F4/80 (macrophages), showing their distribution at the periphery of the islet infiltrate; *b*, stained for relB, showing colocalization with dendritic cells in the islet infiltrate; *c*, for VCAM-1 showing network of dendritic cells in islet infiltrate, and VCAM-1+ activated vascular endothelium (arrowhead).
METHODS. Diabetic mice carrying both the TCR-HNT and Ins-HA transgenes have been described previously. These mice express an islet β-cell-specific transgene antigen (influenza haemagglutinin, or HA) and T-cell receptors specific for HA, and develop early onset spontaneous autoimmune diabetes[27] with infiltrates organized by VCAM-1$^+$ DC[28]. Immunostaining of cryostat sections have been described previously[27]; briefly, cryostat sections of pancreas from the transgenic mice were fixed briefly in 1% paraformaldehyde, incubated with primary antibodies (rat monoclonals F4/80, or anti-VCAM-1 (M/K-2), and rabbit polyclonal anti-RelB (Santa Cruz Biotechnology)), followed by secondary antibodies against the primary (biotin-anti-rat Ig for F4/80 and VCAM-1, followed by avidin peroxidase; peroxidase-conjugated anti-rabbit Ig for the RelB), incubation with amino-ethyl-carbazole (AEC) and haematoxylin counterstain. Magnification, ×160.

‡ To whom correspondence should be addressed.